

MECHANISM OF FIBROUS FRACTURE OF POWDER FORGED STEELS

F. L. Bastian\* and J. A. Charles

Dept. of Metall. and Mat. Science, Univ. of Cambridge  
Pembroke St., Cambridge, England

\*Prog. de Eng. Metal. e Materiais, COPPE/UFRJ (Universidade  
Federal do Rio de Janeiro), Caixa Postal 1191, ZC-00  
Rio de Janeiro, RJ, Brazil

ABSTRACT

The fracture resistance of three steels produced by the powder forging process was evaluated by the Crack Opening Displacement, COD, testing method. The dimple sizes and second-phase particle spacings on the fracture surfaces of the ruptured COD test pieces were assessed using the Scanning Electron Microscope (SEM). The results show that there is a correlation between the oxygen content of the steels and the dimple sizes and particle spacings, insofar as that higher oxygen content are associated to smaller spacings and dimple sizes. The values of COD at initiation,  $(COD)_i$ , are also correlated to those spacings and dimple sizes. A comparison of the obtained results with some published data and with the values of  $(COD)_i$  predicted from the Rice and Johnson model is also made.

KEYWORDS

Powder forged steels, fibrous fracture, fracture toughness, crack opening displacement, fractography, inclusions, dimples.

INTRODUCTION

In the course of a study of the effect of differing deoxidation conditions on the fracture properties of three powder forged steels, a definite correlation was found between their values of Crack Opening Displacement at initiation,  $(COD)_i$ , and oxygen content (Bastian and Charles, 1978). It was also found that the initiation of growth of the fatigue pre-cracks occurred always by the fibrous mechanism, the cracks moving along the prior powder particle boundaries.

The qualitative fractographic analysis performed in that work revealed that there was some sort of relationship between those oxygen content, the dimple sizes and inclusion spacings on the fracture surfaces since higher oxygen content could be associated to smaller spacings and dimple sizes.

These results can be best understood from an analysis of the process of powder forging, where deoxidation during sintering takes place preferentially along the previous powder particle boundaries, due to facility of diffusion along those regions. (Brown, 1976, Ladanyi and others, 1975). As a consequence, the fraction of those previous boundaries occupied by oxide inclusions and their resulting spacings depend



largely on the final oxygen content of the forged material. On the other hand, as the internal oxide inclusions cannot be much affected by the deoxidation treatments, a situation of non-random distribution of inclusions is found in these materials: normally, the spacing of inclusions on prior boundaries is different and smaller than of the internal ones.

It is the purpose of the present work to investigate the relationship between oxygen content, dimple sizes and inclusion spacings on fracture surfaces of powder forged steels. The relationship between these parameters and the  $(COD)_i$  values obtained, is subsequently investigated and the results are compared to the predictions of the model of Rice and Johnson, 1970.

#### MATERIALS

Three steels produced by the powder forging process were studied: a plain carbon steel (M32, commercially known as WP150), a manganese steel (En16) and a Cr, Mn, Ni steel (W32). Three or four different oxygen contents in the steels resulted from differing deoxidation conditions during sintering. The chemical composition of the steels is shown in Table 1 and their final oxygen content in Table 2.

TABLE 1 Chemical Analyses of the Steels Used, wt-%

Steel	C	Mn	Si	S	P	Ni	Cr	Mo	Cu
M32	0.400	0.050	0.050	0.090	0.006	0.070	0.040	0.020	0.100
En16	0.230	0.870	< 0.020	0.018	0.008	0.060	0.050	0.250	0.000
W32	0.245	0.540	< 0.020	0.020	0.013	0.320	0.380	0.340	0.000

TABLE 2 Oxygen Content of Steels Used, wt-%

M32	0.025	0.080	0.100	-
En16	0.029	0.066	0.145	-
W32	0.027	0.075	0.120	0.180

The steels were supplied as discs 69.6 mm in diameter and 15.6 mm in thickness. COD testpiece blanks were cut from the supplied discs as slices 7.0 mm thick which were then heat treated. Heat treatments consisted of oil-quench hardening followed by tempering at 550°C. The resulting Vickers hardness and tensile properties are shown in Table 3.

TABLE 3 Vickers Hardness and Tensile Properties of the Steels Used

Steel	Hardness VH	Yield Stress MNm <sup>-2</sup>	True Stress at maximum load MNm <sup>-2</sup>	Work-hardening Coefficient
M32	202	445	670	0,17
En16	246	614	729	0,13
W32	267	723	833	0,08

#### EXPERIMENTAL METHODS

##### COD Evaluation

The COD testpieces were machined from the fully heat treated blanks and were tested in slow, pure (4 - point) bend. The  $(COD)_i$  values were obtained by the extrapolation method. In this method, extrapolation of the curve COD vs. crack length to zero crack length gives the value of  $(COD)_i$  (Smith and Knott, 1971). Further details of testpiece geometry and test conditions can be found in another work (Bastian and Charles, 1978).

##### Metallography

The mean dimple sizes,  $\bar{D}$ , and the inclusion distributions, characterized by their mean centre to centre spacings,  $|s|_T$ , mean free path,  $|\lambda|_T$ , and average radii,  $|\bar{r}|$ , were estimated from measurements made at very high magnifications (~ 15 Kx) on the fracture surfaces of the ruptured COD testpieces.

A 100 × 100 mm transparent graticule with 100 points, 10 mm spaced, and 10 horizontal lines, each 100 mm long and 10 mm spaced, was superimposed on the CRT screen of a Stereoscan MK II Scanning Electron Microscope. The number of points of the graticule overlapping inclusions were recorded, as well as the number of interceptions of the test lines by inclusions and dimples and the total number of fields measured under the graticule on each specimen. From these data, the values of mean centre to centre spacing, mean free path and average radius of the particles on the fracture surfaces and also the mean dimple sizes were calculated using expressions which can be found elsewhere (Bastian, 1978).

The specimen tilt angle was always 0° and approximately 120 different fields were normally analysed for each composition.

#### RESULTS

The obtained values of mean dimple sizes and mean centre to centre spacing of particles were plotted as function of the oxygen content of the three steels. The resulting curves, Fig. 1 (a) and (b), clearly show an inverse relationship between

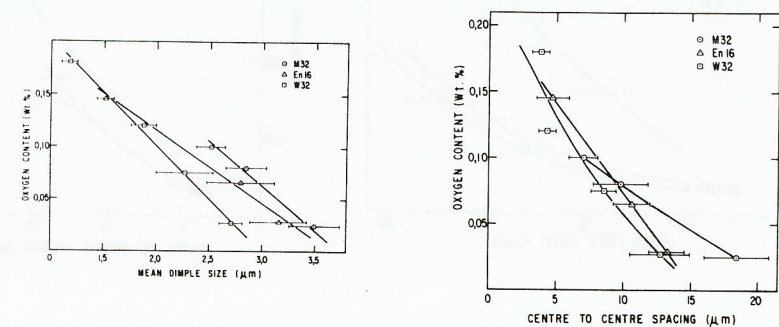


Fig. 1 Oxygen content vs. (a) mean dimple sizes, (b) mean centre to centre spacing of particles

those parameters and the steel oxygen levels, as illustrated by Fig. 2 (a) and (b), which are SEM pictures from the fracture surfaces of the least and most oxidized



compositions of steel M32.

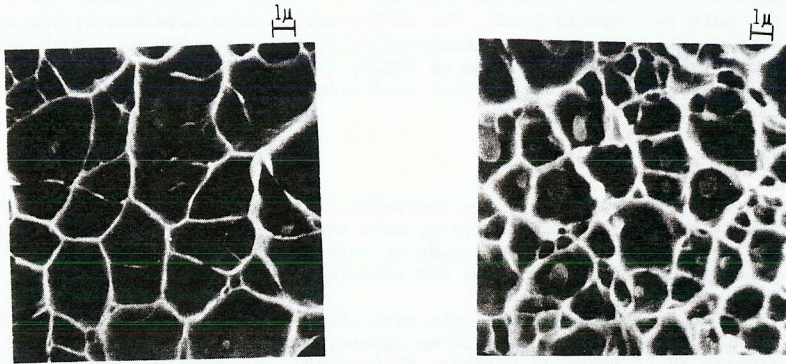


Fig. 2. SEM of fracture surfaces of steel M32, (a) 0.025 wt - % O<sub>2</sub>, (b) 0.100 wt - % O<sub>2</sub>

The values of (COD)<sub>i</sub> obtained were plotted as function of mean free path of particles, Fig. 3 (a), mean centre to centre spacing of particles, Fig. 3 (b), and mean dimple sizes, Fig. 4.

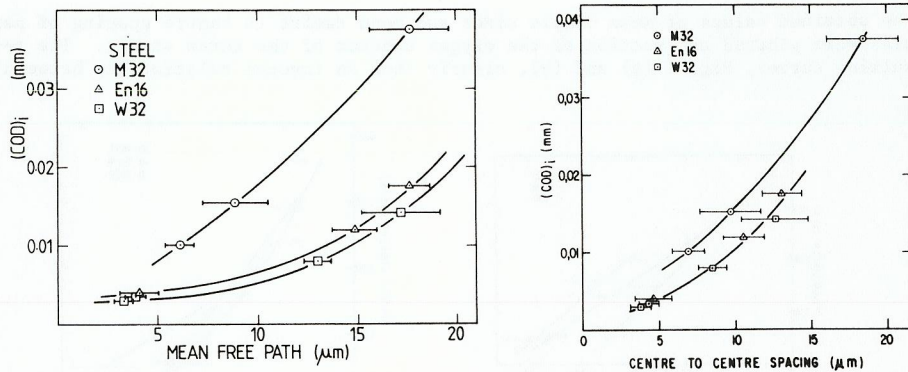


Fig. 3. (COD)<sub>i</sub> vs. (a) mean free path, (b) mean centre to centre spacing of particles

Plots were also made of the ratios of (COD)<sub>i</sub>/|λ<sub>T</sub>| vs. |λ<sub>T</sub>|/|F̄|, (COD)<sub>i</sub>/|s<sub>T</sub>| vs. |s<sub>T</sub>|/|F̄|, Fig. 5, where the curves resulting from the model of Rice and Johnson (1970) are also presented. The values of (COD)<sub>i</sub>/D̄ are shown in Table 4.

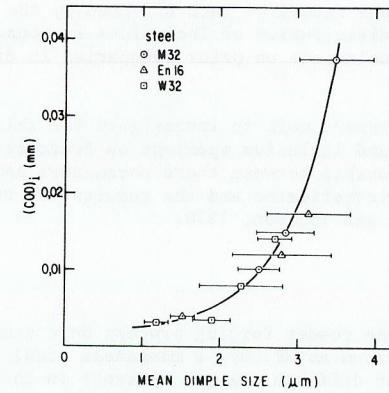


Fig. 4. (COD)<sub>i</sub> vs. mean dimple sizes

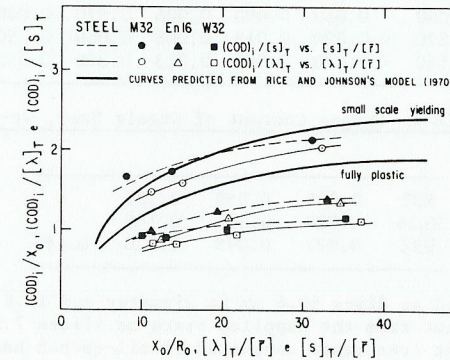


Fig. 5 Ratios of (COD)<sub>i</sub>/spacings vs. spacings/radii

TABLE 4 Ratios (COD)<sub>i</sub>/D̄ of the Steels Studied

Steel	M32	Oxygen wt-%	0.025	0.08	0.10	
		(COD) <sub>i</sub> /D̄	10.75	5.40	4.04	
Steel	En16	Oxygen wt-%	0.027	0.066	0.145	
		(COD) <sub>i</sub> /D̄	5.56	4.29	2.63	
Steel	W32	Oxygen wt-%	0.029	0.075	0.120	0.180
		(COD) <sub>i</sub> /D̄	5.24	3.52	1.86	2.62



## DISCUSSION

Oxygen Content, Particle Spacings and Dimple Sizes

The results clearly show that both particle spacings and dimple sizes depend markedly on the oxygen content of the steels which dictate the amount of oxide inclusions on the prior powder particle boundaries. These are the preferential paths for the ductile crack growth shown by these materials at relatively high oxygen levels (Bastian & Charles, 1978), although crack growth could change to a transparticle path, according to Pillar and others (1977), at some critical low oxygen level. Sources of dimple generation besides the detected particles, like very small oxide, sulphide and carbide particles and, even, possibly, micropores can explain the difference of values of the spacings and dimple sizes, where the dimples are much smaller than the spacings, at any given oxygen level.

A one to one relationship between the inclusion spacings and the dimple sizes was found by Broek (1973) in hot worked aluminium alloys. In that study, thin foils of the materials and replicas of the fracture surfaces of tensile testpieces were analysed using the Transmission Electron Microscope (TEM) which is known to detect the very small particles much better than the SEM. It would be very interesting to use TEM to check whether the one to one relationship mentioned above also holds for powder forged materials where the amount of hot deformation is smaller than in the traditional hot worked materials and where porosity, if incompletely eliminated, may also generate dimples. Inoue and Kinoshita (1973) in a study of a spheroidized carbon steel, using optical microscopy and the SEM, also found a one to one relationship between the above parameters. Careful observation of the figure representing that correlation in their work shows, however, that in the range of larger dimple sizes and carbide spacings, the spacings are larger than the corresponding dimple sizes.

Observation of Fig. 1 in the present work points to the fact that steel M32, although having a higher carbon content, has also larger dimple sizes for any oxygen content, while steel W32 has the smallest ones. This probably results from a finer dispersion on the oxide and carbide particles in steel W32 where the carbides do not coalesce so markedly as the cementite particles at 550°C (Speich and Leslie, 1972). The average size of the particles which were detected by the SEM is the smallest in the case of steel W32 and the largest for steel M32, this probably also happening in the range of sizes which is not detected by this microscope.

(COD)<sub>i</sub>, Particle Spacings and Dimple Sizes

Figs. 3 and 4 show that (COD)<sub>i</sub> is correlated to the mean free path and mean centre to centre spacing to the particles and also to the mean dimple sizes. This is not surprising since a dependence of the spacings and dimple sizes on oxygen content was found in the present work and (COD)<sub>i</sub> was already shown to depend on the oxygen content of the studied steels. An interesting fact emerging from those figures is that three curves result from the plot as function of  $|\lambda|_T$ , two from  $|s|_T$  and one from  $\bar{D}$ . It is also interesting to note that when the average diameter of the detected particles is added to their mean free path, resulting the mean centre to centre spacings, a single curve of (COD)<sub>i</sub> vs.  $|s|_T$  results for the alloyed steels. This situation is maintained in the plot (COD)<sub>i</sub> vs.  $\bar{D}$ , suggesting that the dispersion of the dimple sources which are not detected by the SEM is similar for both alloyed steels. The curve (COD)<sub>i</sub> vs.  $\bar{D}$  of steel M32 is also coincident with the curve of the other steels although different in the plot of (COD)<sub>i</sub> vs.  $|s|_T$ . This probably results from the fact that for a given mean centre to centre spacing of the detected particles, there are more undetected particles in the case of the alloyed steels, causing therefore a translation of their curve of (COD)<sub>i</sub> vs.  $|s|_T$  to larger values of  $|s|_T$ .

These findings could suggest that  $\bar{D}$  is the microstructural parameter to be correlated to (COD)<sub>i</sub> since any given value of  $\bar{D}$  is associated to a single value of (COD)<sub>i</sub>,

independently of the steel composition.  $\bar{D}$  also encloses all sources of void generation, not only second-phase particles but also micropores.

Observation of Fig. 5 and Table 4, on the other hand, shows that the values of (COD)<sub>i</sub>/ $|s|_T$  vs.  $|s|_T/|\bar{r}|$  are the closest to the values predicted from the Rice and Johnson's model (1970), where  $X_0$  is the mean random spacing and  $R_0$  the average radius of the inclusions. The values of (COD)<sub>i</sub>/ $|s|_T$  of the alloyed steels are, however, slightly lower than the corresponding values of (COD)<sub>i</sub>/ $X_0$  from the theoretical curves, for any value of the ratio spacing/radius. This trend is also found in the literature, Knott (1977) and McMeeking (1977), where the ratios of (COD)<sub>i</sub>/spacing tend to be lower than the theoretical ones.

The above comparison was made because the Rice and Johnson's is, at the moment, a very convincing model for expressing crack tip ductility as function of microstructure, as well as good agreement has been observed by several authors between experimental results and the values from the model (Chipperfield, 1973, McMeeking, 1977, Knott, 1977).

Comparison of Fig. 5 and Table 4 shows that the values of (COD)<sub>i</sub>/ $\bar{D}$  are much larger than any theoretical values of (COD)<sub>i</sub>/spacing or the experimentally obtained ones.  $\bar{D}$  was said to enclose all sources of void generation whereas the mean centre to centre spacings of the present work measure the distances of the relatively large particles, detected by the SEM. The good approximation between the values of the curves (COD)<sub>i</sub>/spacings vs. spacings/radii obtained in this work, the theoretical predictions and the available data suggests therefore that the spacing of the large second-phase particles dictates the values of (COD)<sub>i</sub>. These are the critical values of (COD) at which propagation of the cracks initiates. The propagation of the cracks should then take place by the coalescence of voids along those particles, the very small ones and some casual micropores, this generating the final small dimples.

## CONCLUSIONS

The dimple sizes and second-phase particle spacings on the fracture surfaces of the ruptured COD testpieces are inversely related to the oxygen content of the three powder forged steels studied.

The values of (COD)<sub>i</sub> obtained can be correlated to the dimple size and second-phase particle spacings on the fracture surfaces, in such a way that larger spacings and dimples are associated to higher (COD)<sub>i</sub> values.

The results of this work concerning the values of (COD)<sub>i</sub> as function of mean centre to centre spacing and average radius of inclusions on the fracture surfaces are similar to the theoretical predictions by Rice and Johnson as well as to the experimental published data. It is important to note, however, that the other published data involve (COD)<sub>i</sub> as function of mean random spacing and radius measured on polished surfaces.

## ACKNOWLEDGEMENT

The authors wish to thank Professor K.W.K. Honeycombe for making available the necessary research facilities. Financial support from the Conselho Nacional de Desenvolvimento Científico e Tecnológico do Brazil (CNPq) and STI/MIC is gratefully acknowledged by F.L.B.. Without the practical help of GKN Ltd in supplying the whole range of steels tested as sintered and forged blanks, the work would not have been possible. For this, and for the continuing interest and advice of Mr G.T. Brown of GKN we are most appreciative.



## REFERENCES

- Bastian, F. L., and Charles, J. A. (1978). Powder Metall., 4, 199-208.
- Bastian, F. L., (1978). Ph.D. Thesis, University of Cambridge.
- Broek, D., (1973). Eng. Fract. Mech. 5, 55-66.
- Brown, G. T. (1976). Metals Tech., 229-236.
- Chipperfield, C. G. (1973). Ph.D. Thesis, University of Cambridge.
- Inoue, T. and Kinoshita, S. (1973). The Microstructure and Design of Alloys, Proc. Instn. Met., Paper 32, 1, 159.
- Knott, J. F. (1977). Fracture 1977, Vol. 1, ICF4, Waterloo, Canada, 61-92.
- Ladanyi, T. J., Meyers, G. A., Pilliar, R. M. and Weatherly, G. C. (1975). Metall. Trans. 6A, 2037-2048.
- McMeeking, R. M. (1977). J. Mech. Phys. Solids, 25, 357-381.
- Pilliar, R. M., Bratina, W. J. and Blackwell, R. A. (1977), Fracture 1977, Vol. 1, ICF4, Waterloo, Canada, 19-24.
- Rice, J. R. and Johnson, M. A. (1970). Inelastic Behavior of Solids, Kanninen et al., ed. McGraw Hill, 649-661.
- Smith, R. F. and Knott, R. F. (1971). Practic. Applic. of Fract. Mech. to Pressure Vessel Tech., Instn. Mech. Eng. Conf., 65-75.
- Speich, G. R. and W. C. Leslie (1972). Metall. Trans. 3, 1043-1054.